Assimilation of repeated woody biomass observations constrains decadal ecosystem carbon cycle uncertainty in aggrading forests

AGU PUBLICATIONS

JGR

Journal of Geophysical Research: Biogeosciences

RESEARCH ARTICLE

10.1002/2016JG003520

Key Points:
- Improved constraint on retrieved ecosystem traits governing photosynthate allocation and transit times with repeat woody biomass information
- Assimilation of repeat woody biomass information improves constraint on stock and dynamics of independent estimates of dead organic carbon
- The CARDAMOM framework generates estimates of photosynthesis and ecosystem respiration consistent with independent field observations

Supporting Information:
- Supporting Information S1
- Figure S1
- Figure S2

Correspondence to:
T. L. Smallman,
t.l.smallman@ed.ac.uk

Citation:
Smallman, T. L., J.-F. Exbrayat, M. Mencuccini, A. A. Bloom, and M. Williams (2017), Assimilation of repeated woody biomass observations constrains decadal ecosystem carbon cycle uncertainty in aggrading forests, *J. Geophys. Res. Biogeosci., 122*, 528–545, doi:10.1002/2016JG003520.

Received 27 JUN 2016
Accepted 22 FEB 2017
Accepted article online 27 FEB 2017
Published online 11 MAR 2017

Assimilation of repeated woody biomass observations constrains decadal ecosystem carbon cycle uncertainty in aggrading forests

T. L. Smallman[1,2], J.-F. Exbrayat[1,2], M. Mencuccini[1,3], A. A. Bloom[4], and M. Williams[1,2]

[1]School of GeoSciences, University of Edinburgh, Edinburgh, UK, [2]National Centre for Earth Observation, University of Edinburgh, Edinburgh, UK, [3]ICREA at CREAF, Cerdanyola del Valles, Spain, [4]Jet Propulsion Laboratory, California Institute of Technology, Pasadena, California, USA

Abstract Forest carbon sink strengths are governed by plant growth, mineralization of dead organic matter, and disturbance. Across landscapes, remote sensing can provide information about aboveground states of forests and this information can be linked to models to estimate carbon cycling in forests close to steady state. For aggrading forests this approach is more challenging and has not been demonstrated. Here we apply a Bayesian approach, linking a simple model to a range of data, to evaluate their information content, for two aggrading forests. We compare high information content analyses using local observations with retrievals using progressively sparser remotely sensed information (repeated, single, and no woody biomass observations). The net biome productivity of both forests is constrained to be a net sink with <2 Mg C ha^{-1} yr^{-1} variation across the range of inputs. However, the sequestration of particular carbon pool(s) varies with assimilated biomass information. Assimilation of repeated biomass observations reduces uncertainty and/or bias in all ecosystem C pools not just wood, compared to analyses using single or no stock information. As verification, our repeated biomass analysis explains 78–86% of variation in litter dynamics at one forest, while at the second forest total dead organic matter estimates are within observational uncertainty. The uncertainty of retrieved ecosystem traits in the repeated biomass analysis is reduced by up to 50% compared to analyses with less biomass information. This study quantifies the importance of repeated woody observations in constraining the dynamics of both wood and dead organic matter, highlighting the benefit of proposed remote sensing missions.

1. Introduction

Forests are a critical component of the global carbon cycle [*Luyssaert et al.*, 2010], storing significant amounts of carbon (861±66 Pg C), split between living biomass and dead organic matter (including fine litter, coarse woody debris (CWD), and soil organic matter) [*Pan et al.*, 2011; *Liu et al.*, 2015; *Magnusson et al.*, 2016]. There are large carbon fluxes into and out of forests, dominated by natural processes of photosynthesis, respiration, and decomposition, which have a high climate sensitivity, varying in space and time [*Luyssaert et al.*, 2010; *Pan et al.*, 2011; *Magnusson et al.*, 2016]. Forests are also subject to significant impacts from management and other disturbances; consequently, forests may not be in steady state [*Jarvis et al.*, 2009; *Pan et al.*, 2011; *Liu et al.*, 2015; *Poorter et al.*, 2016]. Overall, the carbon budget of forests is the most uncertain component of the global carbon cycle—it is currently impossible to accurately quantify the carbon source/sink strength of forest biomes due to their spatiotemporal heterogeneity and complex dynamics [*Carvalhais et al.*, 2014; *Friend et al.*, 2014].

The storage of woody biomass is determined by the allocation of photosynthate into woody tissue and its turnover (or transit time as defined by *Sierra et al.* [2016]); both of these processes are poorly constrained [*Smith et al.*, 2013; *Malhi et al.*, 2015; *Poorter et al.*, 2016] resulting in large errors in simulated biomass [*Jiang et al.*, 2015]. The transit time of woody biomass is measured in decades but can be highly variable across species, according to disturbance and management regime [*Luyssaert et al.*, 2007; *Malhi et al.*, 2015]. Similarly, the inputs to and transit time of CWD and soil carbon are poorly constrained resulting in large uncertainties in the dynamics and magnitude of these large carbon pools [*Brovkin et al.*, 2012; *Todd-Brown et al.*, 2013; *Exbrayat et al.*, 2014a]. It has been a major challenge to generate robust carbon budgets across landscapes due to data scarcity, e.g., CWD, soil, and woody carbon stocks. Terrestrial ecosystems models (TEM) have been used

for estimating carbon budgets [e.g., *Le Quéré et al.*, 2015], but outputs typically lack an assessment of model uncertainty and exhibit orders of magnitude differences in stock sizes, making a robust assessment of their reliability and precision challenging. TEM-based analyses also typically assume that forests are undisturbed and in steady state with past climate (i.e., model spin-up), which may be inappropriate due to disturbance, either natural or human driven. Moreover, errors in the model spin-up strongly correlate with simulation of carbon stock dynamics [*Exbrayat et al.*, 2014b; *Tian et al.*, 2015].

Now novel data sources such as satellite-based remotely sensed estimates of forest cover and biomass [*Saatchi et al.*, 2011; *Hansen et al.*, 2013; *Thurner et al.*, 2014; *Avitabile et al.*, 2016], plant trait databases [*Wright et al.*, 2004; *Kattge et al.*, 2011], and digitized management [e.g., *National Forest Inventory*, 2011a] and soil maps (Harmonized World Soil Database, HWSD) [*Hiederer and Kochy*, 2011] provide opportunities to generate robust, high-resolution, and spatially continuous and explicit information at landscape scales. However, remotely sensed biomass estimates and soil inventories are typically available with poor temporal resolution [e.g., *Saatchi et al.*, 2011] and/or covering a single ecosystem type [e.g., *Thurner et al.*, 2014], although this is expected to change with the advent of new remotely sensed products generating multiannual information [e.g., *Le Toan et al.*, 2011]. Thus, several distinct combinations of data are likely to be available over different spatial and temporal domains which need to be assessed. Data assimilation techniques can be used to combine such disparate, but spatially explicit, information streams with a process model to produce spatially explicit, temporally constrained analyses of carbon budgets and estimation of ecosystem traits [*Kuppel et al.*, 2012; *Bloom and Williams*, 2015; *Bloom et al.*, 2016].

Remotely sensed biomass estimates will likely provide similar information content to that of field-based (in situ) estimates. The impact of assimilating any given observation is related to its associated uncertainty; field-based estimates of woody biomass have uncertainties of 20–25% [e.g., *Black et al.*, 2009]. Existing remotely sensed biomass products have uncertainties which are highly variable between pixels and between products, e.g., 6–53% tropical biomass [*Saatchi et al.*, 2011] and 20–40% for Northern Hemisphere Boreal forests [*Thurner et al.*, 2014]. However, the pixel level uncertainty of future remotely sensed estimates from the European Space Agency (ESA) Biomass mission is expected to be ~20% [*Le Toan et al.*, 2011].

Here we quantify the information content of management data (i.e., planting dates), biomass estimates, and soil map data for constraining carbon budgets and ecosystem traits of nonsteady state (i.e., aggrading) forests over multiple decades. Our key science question is the following: to what extent are (1) fluxes, (2) stocks of carbon, and (3) ecosystem traits for dynamic systems constrained by management and biomass information? This study lays the foundations for upscaling from site to regional and global scale analyses, generating spatially explicit and dynamic analyses of global forest resources at fine spatial resolutions, utilizing spatially and temporally explicit data sets from existing and upcoming missions for forest biomass mapping [e.g., *Le Toan et al.*, 2011; *Hansen et al.*, 2013; *Thurner et al.*, 2014]. The novelty of this research is that we provide the first quantitative assessment of decadal constraints on forest carbon dynamics arising combining biomass, soil carbon, and management data.

2. Materials and Methods

We carry out data assimilation analyses to address our science question at two well-studied managed evergreen forests—Duke Forest (Loblolly pine, *Pinus taeda*) in the U.S. and Harwood Forest (Sitka spruce, *Picea sitchensis*) in the UK. These sites were chosen because they represent key forestry species in their respective countries and are intensively managed with extensive data sets available with which to constrain and validate their analyses. Loblolly pine plantations covered an area of ~33 million ha or ~16% of the total forest plantation area of the U.S. in 1997 [*Carter and Foster*, 2006; *US Forest Service*, 2001], while Sitka spruce plantations covered an area of ~682,000 ha or ~23% of UK forestry in 2010 [*National Forest Inventory*, 2011a, 2011b].

We use a simple carbon cycle model (DALEC) [*Williams et al.*, 2005; *Bloom and Williams*, 2015], within the CARbon DAta MOdel fraMework (CARDAMOM) framework [*Bloom et al.*, 2016], to assimilate a range of remotely sensed, database, and in situ information using a Metropolis-Hastings Markov Chain Monte Carlo (MH-MCMC) algorithm. CARDAMOM uses spatially and temporally explicit meteorological drivers and carbon cycle observations to generate unique location-specific carbon cycle analyses. We assimilate all available in situ live biomass carbon stock information plus soil organic carbon stock information for Duke and Harwood Forests independently to generate our most data-constrained analysis of their carbon cycles (henceforth referred to as the *Reference* analysis). The Reference analysis provides a baseline against which to assess the information loss to our analyses as in situ carbon stock and management information is progressively removed,

Table 1. Combinations of Data Streams Utilized in the Data Availability Experiments[a]

Experiment	Planting Date	C_{foliar}	C_{root}	C_{wood}	C_{som}	HWSD C_{som} Prior
Reference	Y	Y	Y	Y	Y	N
MultiWood	Y	N	N	Y	N	Y
OneWood	Y	N	N	maximum estimate only	N	Y
ManOnly	Y	N	N	N	N	Y
NoMan	N	N	N	N	N	Y

[a] All scenarios use a time series of LAI to constrain the dynamics of the C_{foliar} pool. Y, Yes; N, No.

ultimately leaving only information in the form of leaf area index (LAI) and a prior estimate of soil carbon derived from the Harmonized World Soil Database (HWSD) [*Hiederer and Kochy*, 2011]. Here we consider the degradation to the estimates and uncertainty of carbon fluxes and stocks but also to the retrieved ecosystem traits in comparison with field observations. Finally, we validate our analyses using carbon flux estimates from eddy covariance observations and in situ estimates of dead organic matter stocks. The validation information are fully independent and not assimilated in any analysis here.

2.1. Experimental Design

2.1.1. Data Availability Scenarios

The data availability scenarios address combinations of ecosystem carbon stock data which are likely to be available either currently or in the near future (Table 1). All scenarios assimilate a time series of LAI. At Duke Forest the LAI time series are derived from in situ observations [*McCarthy et al.*, 2010]. At Harwood Forest only four LAI estimates are available; therefore, to provide continuous time series information, the in situ observations have been used to bias correct Moderate Resolution Imaging Spectroradiometer (MODIS) LAI (2001–2008, MOD15A2 LAI-8 day version 5, 1 km resolution product, http://lpdacc.usgs.gov/, using the maximum quality flagged information only). Each scenario except Reference also uses a prior estimate of the initial soil carbon stock derived from the HWSD [*Hiederer and Kochy*, 2011]. The HWSD-derived prior estimates for soil carbon are 82 Mg C ha^{-1} for Duke Forest and 218 Mg C ha^{-1} for Harwood Forest. The HWSD information is nominally assumed to represent the top 1 m of soil.

Five data availability scenarios have been analyzed at each site in approximate decreasing order of in situ information content (Table 1). The Reference analysis assimilates all in situ information on foliage, fine root, wood (combining stem, branch, and coarse root), and soil carbon stocks. Note that the combination of LAI and in situ information on the foliar carbon stock also constrains the leaf carbon mass per leaf area (LCMA). Location-specific information on fine root, foliage, and soil carbon stocks are unlikely to be available except for site scale analyses. Therefore, we define two scenarios, *MultiWood* which assimilates multiple in situ wood stock observations and *OneWood* which assimilates the most recent single in situ wood stock observation. In many locations no biomass information is available; therefore, we assess the impact of management information only (i.e., forest age) in the *ManOnly* scenario. The final scenario (*NoMan*) assimilates only data which currently have global spatial coverage (e.g., MODIS LAI and HWSD). This information is required to support upscaling analyses of managed forest carbon dynamics over spatial areas where limited information is available.

The Princeton meteorological reanalysis (1° × 1° spatial resolution) provides air temperature, short-wave radiation, and vapor pressure deficit [*Sheffield et al.*, 2006], while the atmospheric CO_2 concentration was held constant at 380 ppm. The Duke Forest analyses cover a 26 year period from planting in 1983 until the end of 2008. At Harwood Forest a pseudo time series of forest biomass was created using the chronosequence of in situ observations, where the 30 year old stand is placed at the observation date in 2001 and all other observations are placed prior to 2001 based on their age difference from the 30 year old stand (i.e., the 21 year old stand data are placed in 1992). The Harwood Forest analyses cover a 37 year period from 1972 until the end of 2008. All analyses were conducted at a daily time step.

2.1.2. Site Description and Observations: Duke Forest

Duke Forest in North Carolina, U.S. (35.97°N, 79.09°W; elevation 163 m) is a second-rotation uniform age loblolly pine (*Pinus taeda*) plantation with a deciduous hardwood understory. The first rotation was cleared in 1982 and replanted in 1983 on moderately low-fertility acidic clay-loam soil. The mean annual air temperature is 15.8°C, and precipitation is 1145 mm [*McCarthy et al.*, 2007].

Observations were collected at Duke Forest for both the loblolly pine and understory as part of the Duke CO_2 Free Air CO2 Enrichment (FACE) experiment [*Oren et al.*, 2001]; here we use data collected from the unfertilized

Table 2. Uncertainties Assimilated for Globally Available Data and Assumed Uncertainties for Harwood Forest Site Estimates Based on *Black et al.* [2009][a]

Data Stream	Uncertainty
LAI	log(2)
HWSD C_{som} prior	log(2)
C_{foliar}	38%
C_{wood}	25%
C_{root}	44%
C_{som}	24%

[a]A lognormal uncertainty is assumed for LAI and HWSD.

ambient CO_2 plots. Available in situ carbon stock observations are the growing season maximum estimates of foliage, fine root, and wood for each year of 1996–2004 inclusive [*Oren et al.*, 2001; *McCarthy et al.*, 2010] and a single estimate of soil organic carbon in 2005 (0–100 cm [*Lichter et al.*, 2008]). The mean annual wood increment is 4.5 Mg C ha^{-1} yr^{-1}. Observation uncertainty is assumed to be the standard deviation of the plot estimates. Additional observations are available but are not assimilated in any analysis to provide fully independent validation. These data are in situ estimates of forest floor litter for 1996, 1999, 2002, and 2006 (0–15 cm depth [*Lichter et al.*, 2008]) and gross primary productivity (GPP) and ecosystem respiration (R_{eco}) estimates derived from eddy covariance [2001–2004; *Oren et al.*, 2006; *Stoy et al.*, 2006].

2.1.3. Site Description and Observations: Harwood Forest

Harwood Forest in Northumberland, UK (55.21° N, 2.04° W; elevation 200–400 m) consists of even aged stands of Sitka spruce (*Picea sitchensis*) managed on rotations of 40–60 years followed by clear felling. There is no understory present at Harwood Forest. Harwood Forest was established in the 1930s on seasonally saturated peaty gley soil, covering an area of approximately 4000 ha [*Zerva and Mencuccini*, 2005]. The mean annual air temperature is 7.6°C and precipitation is 950 mm.

Data were collected from a chronosequence of four stands aged 3, 8, 21 and 30 years during summer 2001. Stands aged 3 and 8 years are second rotation while stands aged 21 and 30 years are first rotation. The yield class for each stand in the chronosequence is ~6 $m^3 ha^{-1}$ yr^{-1} wood volume increment in the UK Forestry Commission subcompartment database (www.forestry.gov.uk/datadownload, accessed 30/10/2015). Carbon stock estimates for foliage (including an estimate of LCMA), fine root, wood and soil organic matter (0–45 cm) were collected from each stand [*Zerva and Mencuccini*, 2005; *Magnani et al.*, 2007]. We note also that the soil carbon observations here extend to only 45 cm depth while the HWSD estimate nominally represents the top 1 m. However, the impact of this difference is expected to be minimal as the carbon concentration in observations declines by >90% between the surface and 45 cm depth [*Zerva and Mencuccini*, 2005]. None of the chronosequence stands were resampled at a later time from which to estimate the mean annual woody increment. Therefore, the chronosequence stands themselves have been used to create a pseudo time series for which mean annual wood increment is 2.2 Mg C ha^{-1} yr^{-1}. As no estimate of uncertainty is available for these data, we conservatively use the upper estimate of uncertainty from a similar Sitka spruce chronosequence in Ireland (Table 2) [*Black et al.*, 2009]. Additional observations are available to provide fully independent validation. An in situ estimate of total dead organic matter ($C_{DeadOrg}$; i.e., forest floor litter plus CWD) is available for the 30 year old stand (i.e., collected in 2001) and an annual estimate of gross primary productivity (GPP) and ecosystem respiration (R_{eco}) derived from eddy covariance (2001) [*Kowalski et al.*, 2004].

2.2. Independent Validation

We compare each analysis against all available observations irrespective of whether a given datum has been assimilated in a specific analysis, providing a means to assess the degradation of each analysis in the absence of given data. In addition we validate our analyses against fully independent in situ estimates of dead organic matter (i.e., litter and/or CWD) and annual estimates of GPP and R_{eco} derived from eddy covariance. These data are not assimilated in any analysis. Furthermore, we compare our retrieved estimates of ecosystem traits such as the allocation of net primary productivity (NPP) and ecosystem mean transit times (MTT) with literature estimates. Through a combination of validation and corroboration we aim to identify remaining weaknesses and missing process information, due to the use of global data, required for future studies.

2.3. Analysis Framework

2.3.1. C Cycle Model

DALEC simulates the daily ecosystem carbon balance representing carbon stocks and fluxes between labile (C_{labile}), foliage (C_{foliar}), fine root (C_{root}), wood (C_{wood}; including branch, stem and coarse root), litter (C_{litter}),

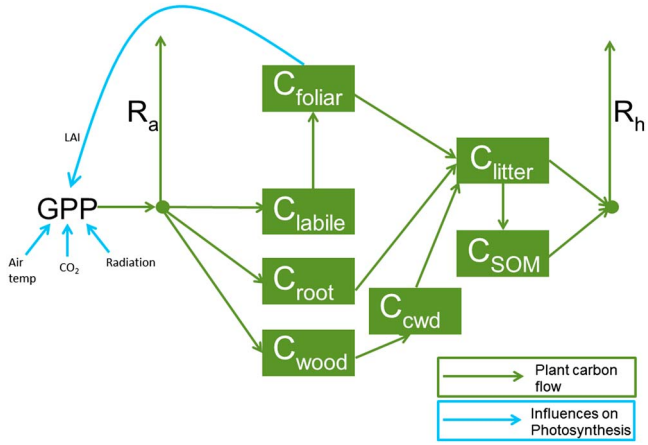

Figure 1. Schematic of the DALEC model. Green arrows indicate biosphere carbon flows. The blue arrows show the inputs to the photosynthesis model. R_a is autotrophic respiration while R_h is heterotrophic respiration.

coarse woody debris (C_{cwd}), and soil organic matter (C_{som}) (Figure 1) [*Bloom et al.*, 2016]. Gross primary productivity (GPP) is calculated using the aggregated canopy model (ACM) [*Williams et al.*, 1997]. GPP is then allocated based on fixed fractions, while C pool turnover follows first-order kinetics. Canopy phenology is sensitive to environmental drivers via a modified version of the growing season index model (GSI model) [*Jolly et al.*, 2005; *Stoeckli et al.*, 2008]. A C_{cwd} pool has been added to our version of DALEC due to the necessity of distinguishing between nonwoody (C_{litter}) and woody litter (C_{cwd}) to improve the analysis of decomposition processes [*Brovkin et al.*, 2012]. Here the inclusion of C_{cwd} prevents the unrealistic accumulation of new soil organic matter found when using previous versions of DALEC. See Text S1 of the supporting information for details.

The data assimilation analysis retrieves a total of 30 parameters for DALEC; 23 parameters govern ecosystem processes, while the remaining 7 parameters describe the initial carbon stocks. Here we focus on the retrieval of information on traits governing the allocation of photosynthate and MTT of ecosystem carbon stocks. We define the MTT as the mean ratio of carbon losses from a given pool relative to the size of the pool.

2.3.2. Data Assimilation Approach

The model-data fusion framework employed here calculates the probability of a given parameter vector x by comparing simulated DALEC stocks and fluxes with spatially and temporally explicit observations. We prescribe a uniform prior probability density function for x between minimum and maximum parameter values ($P_{range}(x)$) (Table 3). Model predictions and observations, and their uncertainties, are compared within a Bayesian framework [*Ziehn et al.*, 2012; *Bloom and Williams*, 2015] to derive a posterior probability density function ($P(x|O)$) of a given parameter vector x.

$$P(x|O) \propto P(O|x) \cdot P_{range}(x) \cdot P_{EDC}(\mathrm{DALEC}(x)) \tag{1}$$

$P(O|x)$ is the probability of the observations given x, $P_{range}(x) = 1$ if all parameters are within predescribed ranges (Table 3), and $P_{EDC}(\mathrm{DALEC}(x)) = 1$ if all Ecological and Dynamical Constraints (EDCs) criteria are achieved. $P(O|x)$ is derived from available observations, their uncertainty and model state variables simulated from a given x.

$$P(O|x) = e^{-0.5 \cdot \sum_{n=1}^{N} (M_n - O_n)^2 / \sigma_n^2} \tag{2}$$

O_n is the nth observation, and M_n is the corresponding model state variable or flux. Each observation has an associated error variance (σ_n^2); note that we assume that there is no covariance between observation errors and M_n and O_n are log transformed for LAI and HWSD, which we assume have lognormal uncertainties [*Bloom and Williams*, 2015]. If $P_{range}(x)$ or $P_{EDC}(\mathrm{DALEC}(x)) = 0$ then x is rejected irrespective of $P(O|x)$.

The EDCs are employed to improve realism of parameter selection and, as a result, lead to a reduction in parameter uncertainty and bias [*Bloom and Williams*, 2015]. If $P_{EDC}(\mathrm{DALEC}(x))$ and $P_{range}(x) = 1$, a parameter vector is accepted if its probability is greater than the probability of the last accepted parameter vector. Should the probability of a parameter vector not be greater than the previous accepted vector, it is still accepted if the ratio between its probability and the last accepted probability is less than a random number selected from a uniform distribution between 0 and 1 (U_{0-1}) [*Ziehn et al.*, 2012; *Bloom and Williams*, 2015].

2.3.3. Ecological and Dynamical Constraints

EDCs ensure that parameter combinations which generate unrealistic stock dynamics and ecologically inconsistent parameter combinations are rejected. The EDCs described in *Bloom and Williams* [2015] have been

Table 3. Descriptions, Units, and Prior Ranges of DALEC Parameters[a]

Description	Units	Minimum Value	Maximum Value
Decomposition of C_{litter} to C_{som} ($Decomp_{litter}$)	g C m^{-2} day^{-1}	1e−5	0.01
Fraction of GPP respired (Ra:GPP)	-	0.3	0.7
Fraction of GPP to C_{labile} (GPP_{lab})	fraction	0.01	0.5
Fraction of GPP to C_{root} (GPP_{root})	fraction	0.01	1.0
Maximum C_{foliar} turnover (k_{fol})	fraction day^{-1}	1e−6	0.2
Maximum C_{labile} turnover (k_{lab})	fraction day^{-1}	1e−6	0.2
Turnover of C_{wood} (θC_{wood})	fraction day^{-1}	1e−5	0.001
Turnover of C_{root} (θC_{root})	fraction day^{-1}	1e−4	0.01
Turnover of C_{cwd} (θC_{cwd})	fraction day^{-1}	1e−4	0.01
Mineralization of C_{litter} (θC_{litter})	g C m^{-2} day^{-1}	1e−4	0.01
Mineralization of C_{som} (θC_{som})	g C m^{-2} day^{-1}	1e−7	0.001
Heterotrophic respiration exponential temperature response (Rh_{temp})	-	0.018	0.08
Canopy photosynthetic efficiency (Ceff)	g Cm^{-2} day^{-1} at 0°C	10	100
Leaf carbon mass per leaf area (LCMA)	g C m^{-2}	10	200
GSI minimum temperature threshold ($mtemp_{min}$)	K	225	330
GSI maximum temperature threshold ($mtemp_{max}$)	K	225	330
GSI minimum photo period threshold ($photop_{min}$)	h	1	12
GSI maximum photo period threshold ($photop_{max}$)	h	1	18
GSI minimum VPD threshold (VPD_{min})	Pa	1	5,500
GSI maximum VPD threshold (VPD_{max})	Pa	1	5,500
GSI critical GPP increase for additional C_{labile} turnover (β GPP)	fraction	1e−10	0.2
GSI climate sensitivity for C_{labile} turnover (β GSI_{lab})	-	−0.05	0.05
GSI climate sensitivity for C_{foliar} turnover (βGSI_{fol})	-	−0.05	0.05
Initial C_{labile} pool size	g C m^{-2}	1	1,000
Initial C_{foliar} pool size	g C m^{-2}	1	1,000
Initial C_{root} pool size	g C m^{-2}	1	1,000
Initial C_{wood} pool size	g C m^{-2}	1	20,000
Initial C_{cwd} pool size	g C m^{-2}	1	10,000
Initial C_{litter} pool size	g C m^{-2}	1	10,000
Initial C_{som} pool size	g C m^{-2}	100	200,000

[a]All parameter ranges are as presented in *Bloom and Williams* [2015] except those governing the GSI model which are based on those found in *Stoeckli et al.* [2008]. $Decomp_{litter}$, θC_{litter}, and θC_{som} are baseline values adjusted by an exponential function of temperature. GPP allocation fractions are applied sequentially such that GPP allocation to C_{wood} = GPP − (*GPP·Ra:GPP) − (GPP·GPP_{lab}) − (GPP·GPP_{root}).

modified to include additional prior knowledge appropriate for managed forest systems and to ensure realistic parameter combinations for the phenology model. EDC modifications include additional constraint to the accepted C_{root}:C_{foliar} [*Albaugh et al.*, 2004; *Black et al.*, 2009; *Morison et al.*, 2012; *Akers et al.*, 2013] and reformulation of C_{foliar} turnover rates to include the impact of the phenology model. New EDCs include placing an upper limit on the C_{labile}:C_{wood} ratio and C_{labile} MTT consistent with literature estimates [*Samuelson et al.*, 2004; *Gough et al.*, 2009; *Richardson et al.*, 2013a, 2015]. Finally, an EDC governing the expected biomass at the beginning of the analysis based on yield curve estimates for a given forest stand age is used to provide additional constraint on the initial conditions. The yield curve estimates are based on forestry yield curves [*Randle and Jenkins*, 2011]; however, no yield class information is used here, instead relying on the maximum and minimum possible values at a given age across all yield classes. Detailed description of the EDCs can be found in Text S2 of the supporting information.

3. Results

All analyses of forest carbon cycling, at both sites, are consistent with the assimilated in situ biomass and management information. The analyses constrain the mean annual net biome productivity ($\overline{NBP}$) of both forests

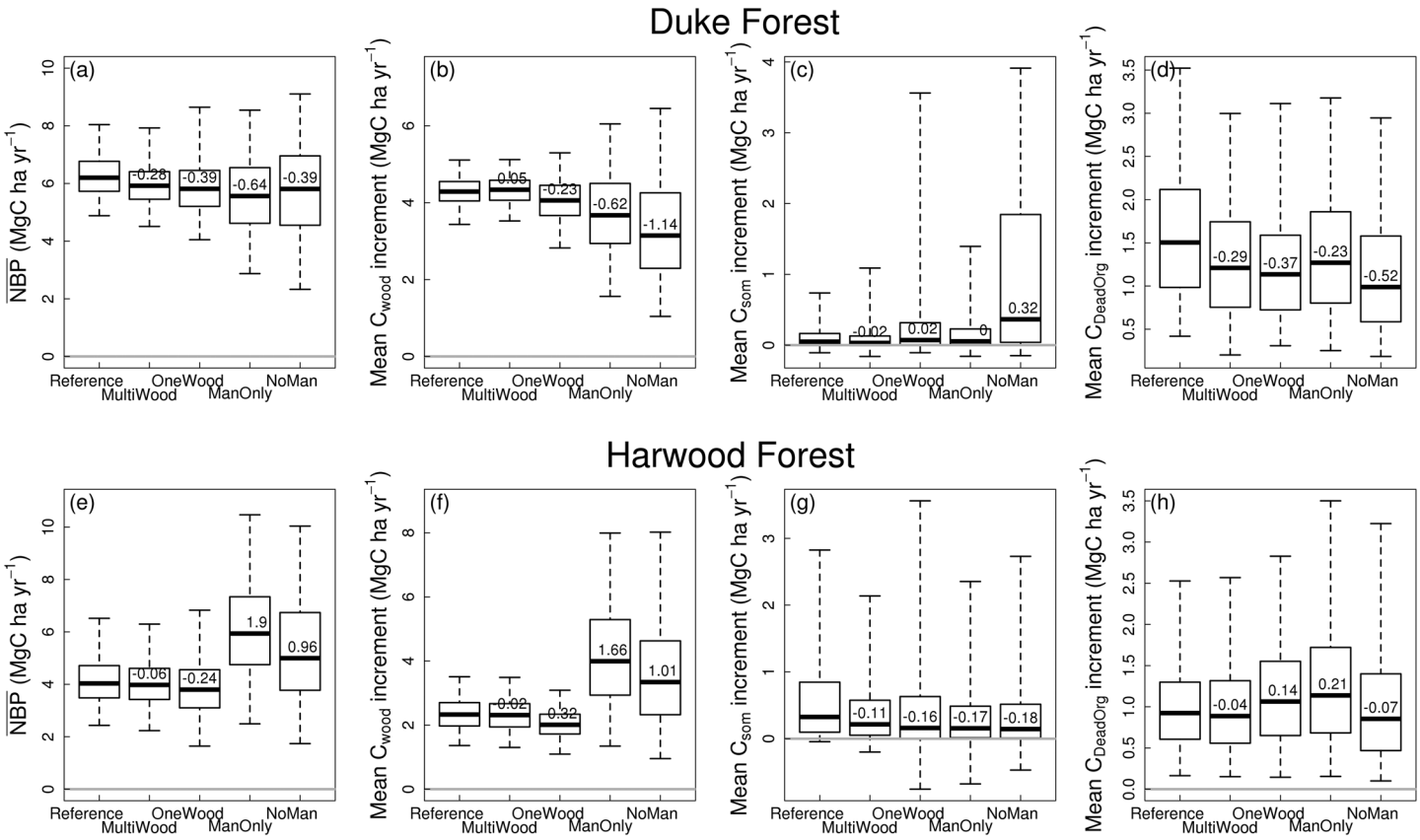

Figure 2. Box and whisker plots show the median and distribution information retrieved for (a, e) the mean annual net biome productivity ($\overline{NBP}$), and the mean annual accumulation of (b, f) C_{wood}, (c, g) C_{som}, and (d, h) $C_{DeadOrg}$. A positive value indicates a net accumulation of carbon within the forest or carbon pool. The median is shown by the thick black horizontal line, while the box and whiskers represent the 50% and 95% confidence intervals, respectively. The number imposed on each graph is the bias between the Reference analysis and the respective data availability scenario. Figures 2a–2d are Duke Forest, and Figures 2e–2h are Harwood Forest.

as clear carbon sinks over their respective analysis periods (Figure 2). Analyses with reduced information show a quantifiable increase in uncertainty and bias in carbon fluxes, stocks, and ecosystem traits at both sites compared to the Reference analysis (Figures 3–8).

The Reference analyses at both sites compare well against independent estimates of annual GPP, R_{eco}, litter (C_{litter}), and dead organic matter ($C_{DeadOrg} = C_{litter}+C_{cwd}$). The root-mean-square error (RMSE) of annual GPP (2001–2005) at Duke Forest is 386 g C m^{-2} yr^{-1} (18% of the observed estimate), while at Harwood Forest the RMSE for annual GPP (2001) is 486 g C m^{-2} yr^{-1} (24%). The RMSE for R_{eco} at Duke Forest is 191 g C m^{-2} yr^{-1} (11%), and at Harwood Forest the RMSE is 471 g C m^{-2} yr^{-1} (34%). The uncertainties for the eddy covariance estimates and our analysis here overlap in each case except GPP in 2001–2002 at Duke Forest, where the separation between uncertainty bounds is <90 g C m^{-2} yr^{-1}. At Duke Forest our analysis explains 56% of daily variation in GPP and R_{eco} with an RMSE of 2.3 g C $m^{-2}day^{-1}$ for GPP and 1.7 g C $m^{-2}day^{-1}$ for R_{eco}. There are no daily time step estimates of GPP or R_{eco} available for Harwood Forest. At Duke Forest the observed litter estimates C_{litter} are well within the analysis uncertainty, and the median estimate explains 79% of year to year variation with an a RMSE of 2.1 Mg C ha^{-1} (22%) (Figure 8a). Finally, at Harwood Forest the combined estimate of forest floor litter and coarse woody debris ($C_{DeadOrg}$) is predicted with an error of 3.8 Mg C ha^{-1} yr^{-1} (12%) (Figure 8c).

3.1. Reference Analysis

3.1.1. C Dynamics

At Duke Forest the median (2.5%/97.5%) $\overline{NBP}$ is estimated to be a net carbon sink of 6.2 (4.9/7.9) Mg C ha^{-1} yr^{-1} (Figure 2a). The majority of carbon at Duke Forest is accumulated in the C_{wood} pool with a mean annual increment of 4.3 (3.5/5.0) Mg C ha^{-1} yr^{-1}, with a further 1.5 (0.5/3.4) Mg C ha^{-1} yr^{-1} accumulating in the

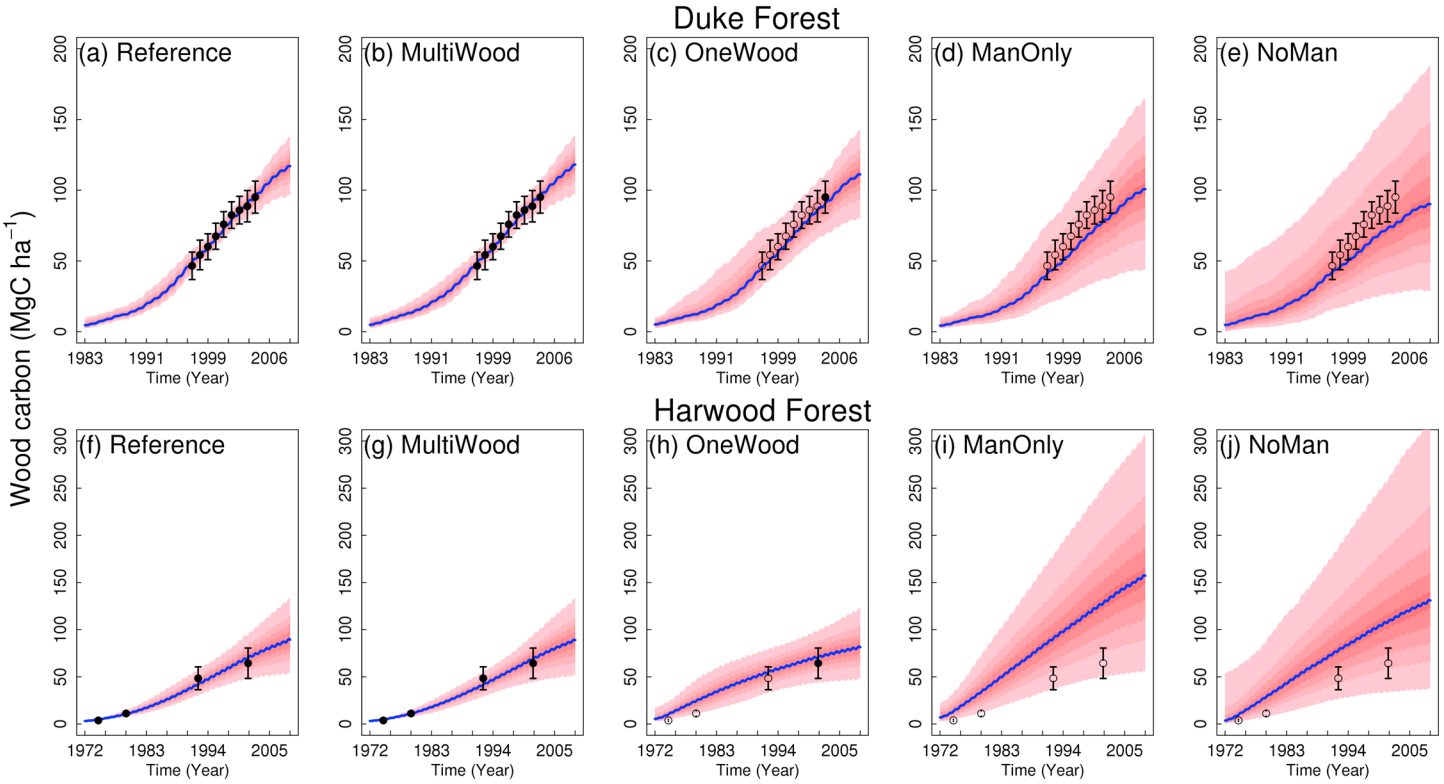

Figure 3. Time series of C_{wood} at (a–e) Duke and (f–j) Harwood Forest showing each analysis, where the assimilated information progressively decreases from left to right. The shaded red area denotes the 95% confidence interval of the analysis ensemble were the blue line is the ensemble median. The filled black circles are assimilated in situ observations, while the unfilled black circles are data shown for reference and not assimilated in a given analysis. The error bars indicate the observation uncertainty assimilated into the analysis.

$C_{DeadOrg}$ and 0.05 (−0.09/0.7) Mg C ha^{-1} yr^{-1} accumulating in the C_{som} pool (Figures 2b–2d). Harwood Forest is also a net carbon sink with a $\overline{NBP}$ of 4.0 (2.6/6.3) Mg C ha^{-1} yr^{-1} (Figure 2d). Similarly, the majority of the net carbon sink at Harwood Forest is accumulated in the C_{wood} pool with a mean annual increment of 2.3 (1.4/3.4) Mg C ha^{-1} yr^{-1}, with 0.9 (0.2/2.3) Mg C ha^{-1} yr^{-1} accumulating in the $C_{DeadOrg}$ and 0.3 (−0.03/2.6) Mg C ha^{-1} yr^{-1} in the C_{som} (Figures 2f–2h). The Reference analysis constrains the $\overline{NBP}$ at both sites to a 95% confidence interval (CR_{95}) range of <3.7 Mg C ha^{-1} (Figures 2a and 2e). At both sites the CR_{95} for the mean annual increment of C_{wood} is <3.5 Mg C ha^{-1}, <3.0 Mg C ha^{-1} for $C_{DeadOrg}$, and <2.6 Mg C ha^{-1} for C_{som} (Figures 2b–2d and 2f–2h).

Assimilated in situ wood stock information at both sites is well captured by the Reference analysis (Figures 3a and 3f). At Duke Forest the RMSE between the Reference analysis and in situ wood stock observations is 2.0 Mg C ha^{-1} with a bias (model-data) of −0.29 Mg C ha^{-1} (Table 4). At Harwood Forest the RMSE is 4.4 Mg C ha^{-1} and the bias is −0.21 Mg C ha^{-1}. The median estimate of C_{som} at Duke Forest accurately simulates the assimilated soil carbon information (Figure 4a), while at Harwood Forest the assimilated soil carbon information are within the analysis 95% confidence interval (CI_{95}) (Figure 4f).

Analysis of the foliar and fine root carbon stocks is more challenging than that of wood or soil carbon particularly at Harwood Forest (Figure 5). At Duke Forest the mean annual peak values in foliar carbon are well captured by the Reference analysis except the peak value in 2001. The retrieved phenology parameters indicate that variation in canopy phenology is dominated by variation in temperature (95 (62/97)%) with the remaining variability due to variation in vapor pressure deficit (VPD). At Harwood Forest the analysis accurately simulates the foliar carbon stock observations for the 9 year old stand (i.e., 1980) but underestimates the foliar stock observations for the 21 and 30 year old stands (1992 and 2001, respectively) by 4–5 Mg C ha^{-1} each (Figure 5c). As the biomass information is constructed from a chronosequence and does not overlay with the MODIS LAI derived time series used here, there is limited scope for interpretation. The bias between the observations and the median estimate of fine roots is less than 0.5 Mg C ha^{-1} yr^{-1} at both Duke and Harwood

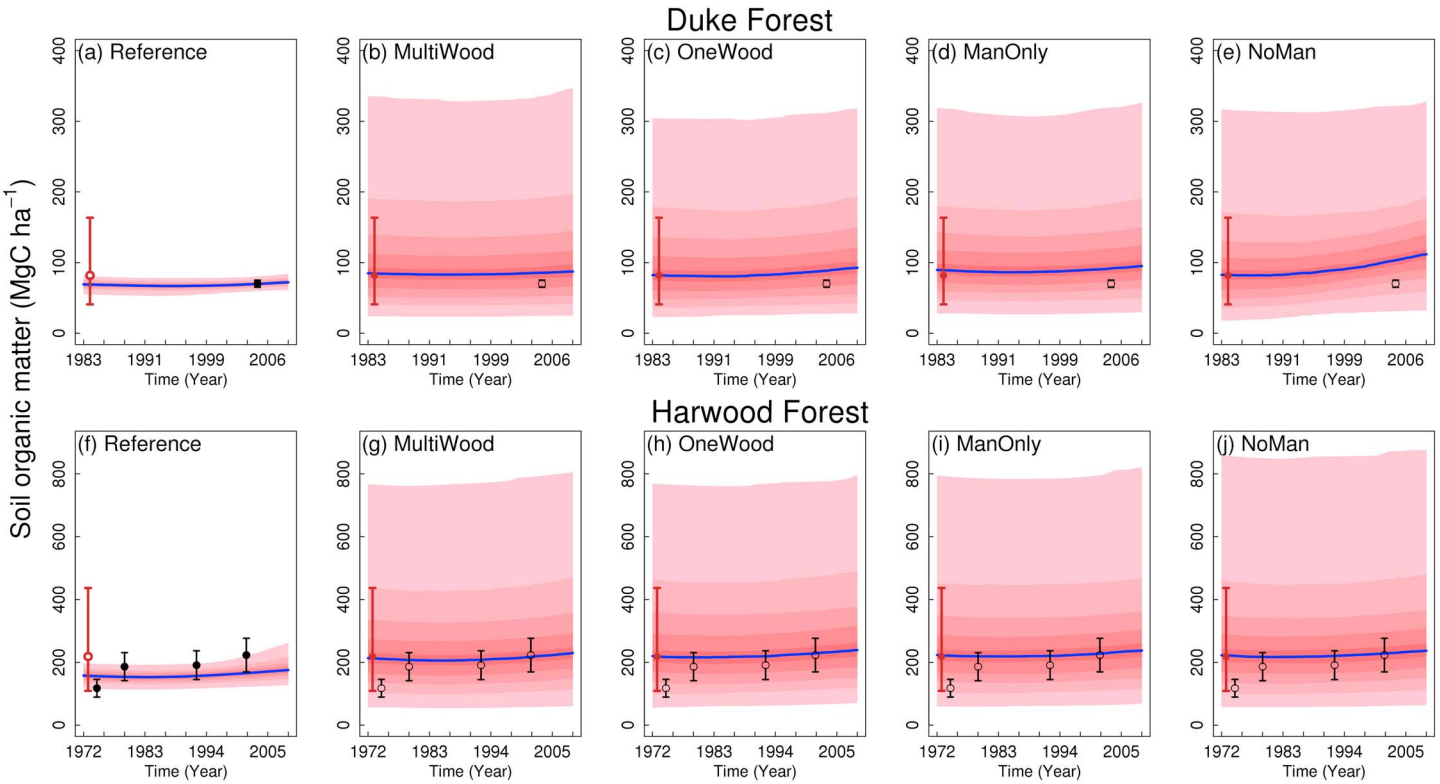

Figure 4. Time series of C_{som} at (a–e) Duke and (f–j) Harwood Forest showing each analysis, where the assimilated information progressively decreases from left to right. The shaded red area denotes the 95% confidence interval of the analysis ensemble, while the blue line is the ensemble median. The filled black circles are in situ observations assimilated in a given analysis, while the unfilled black circles are data shown for reference and not assimilated in a given analysis. The error bars indicate the observation uncertainty assimilated into the analysis. When the brown circle is filled the C_{som} prior, derived from the HWSD, is assimilated into the analysis; when unfilled the C_{som} prior was not assimilated and is shown for reference only.

Forests (Figures 5b and 5d). At Harwood Forest the CI_{95} remains substantial at onefold to fourfold greater than the mean magnitude of in situ observations (~1 Mg C ha^{-1} yr^{-1}).

3.1.2. Retrieved Ecosystem Traits

Retrieved ecosystem traits for the Reference analysis is consistent with expectations based on field observations (Figure 6). The fraction of NPP allocated to C_{wood} is well constrained with a median value of ~0.7 at both Duke and Harwood Forests (Figures 6a and 6e). The Ra:GPP (carbon use efficiency = 1 − Ra:GPP) at Duke Forest is estimated to be ~0.4 and ~0.58 at Harwood Forest (Figures 6d and 6h). The retrieved MTT for C_{wood} (19–22 years) and $C_{DeadOrg}$ (3.5–3.9 years) are also similar between sites (Figures 6b, 6c, 6f, and 6g). However, while the MTT of the C_{cwd} at both sites is similar (7.6–7.9 years), the MTT of C_{litter} at Duke Forest (2.1 (0.2/8.8) years) is more than double that of Harwood Forest (0.8 (0.2/7.9) years). The MTT for C_{som} at Harwood Forest (~275 years) is 48 years longer than Duke Forest (~227 years). Overall retrieval of MTTs remains more uncertain than allocation of NPP (Figure 6). Note also that as DALEC does not explicitly simulate self-thinning, the C_{wood} mean transit times retrieved here implicitly include self-thinning resulting in shorter transit times than might be expected. The median estimate of LCMA at Duke Forest is 90 (76/105) g C m^{-2}, which is consistent with the in situ estimate of 86 (81/90) g C m^{-2} (which in the Reference analysis is implicitly assimilated through the combination of in situ LAI and foliar stocks). At Harwood Forest the retrieved LCMA is more uncertain at 129 (75/191) g C m^{-2}. However, the in situ estimate of LCMA at Harwood Forest varies with stand age; LCMA estimates are 97, 166, and 167 g C m^{-2} for stands aged 9, 21, and 30 years, respectively. Therefore, the increased uncertainty in retrieved LCMA at Harwood Forest accurately captures the variation of the in situ observations. The CI_{95} of the retrieved posterior distributions of ecosystem traits for the Reference analysis differ between sites. At Duke Forest the parameter posterior distributions are on average 45% smaller than in NoMan (Figure 7a), while at Harwood Forest the mean parameter posterior is 24% smaller than in NoMan (Figure 7b). However, the overall pattern of improved constraint when considering parameters related to distinct process areas is consistent between sites. At both sites parameters related to MTTs have the smallest

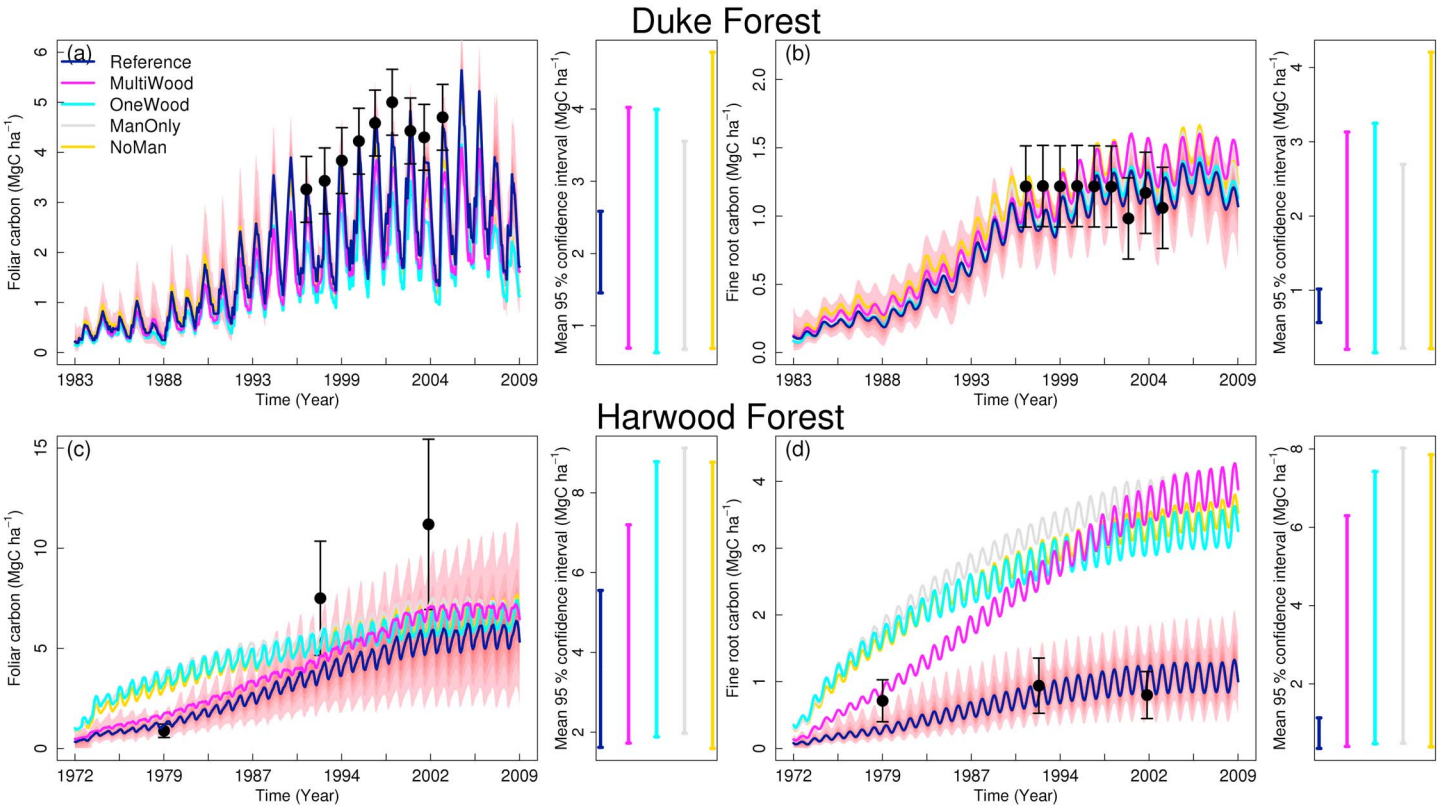

Figure 5. Time series of (a, c) C_{foliar} and (b, d) C_{root} for Duke (Figures 5a and 5b) and Harwood Forests (Figures 5c and 5d). The shaded red area denotes the 95% confidence interval of the Reference analysis. The lines on the large panels are the ensemble medians for each of the data availability experiments. The error bars shown in the small panels are the mean 95% confidence intervals for each experiment over the analysis period. The filled black circles are in situ observations assimilated in Reference analysis only, and error bars indicate the observation uncertainty.

increase in constraint relative to NoMan, while initial conditions have the greatest increase in constraint relative to NoMan. A complete list of parameter uncertainty reductions for each data availability scenario is available in Tables S1 and S2.

3.2. Impact of Reducing Information on Carbon Retrievals

3.2.1. C Fluxes

The $\overline{NBP}$ and its CI_{95} at both sites are sensitive to reducing the quantity of assimilated biomass information. At Duke Forest the removal of in situ foliar, fine root, and soil carbon stock information in MultiWood has a small impact on the $\overline{NBP}$ (0.29 Mg C ha^{-1} yr^{-1}) and its CI_{95} (5%) (Figure 2a). The removal of all but one in situ wood stock observation in the OneWood analysis increases the $\overline{NBP}$ bias with the Reference analysis to −0.39 Mg C ha^{-1} yr^{-1} (i.e., an underestimate), and the CI_{95} increases by 42%. The removal of all in situ carbon stock information in the ManOnly analysis increases the CI_{95} by 73% relative to the Reference analysis, and the $\overline{NBP}$ bias increases to its largest magnitude of −0.64 Mg C ha^{-1} yr^{-1} (Figure 2a). With the removal of forest age information in NoMan the CI_{95} of $\overline{NBP}$ more than doubles (113%) relative to the Reference analysis, though the bias decreases to that found in OneWood. At Harwood Forest the $\overline{NBP}$ responds similarly to the removal of in situ foliar, fine root, soil carbon, and multiple wood stock estimates. However, once all in situ biomass information is removed in ManOnly the $\overline{NBP}$ bias increases to 1.9 Mg C ha^{-1} yr^{-1} (i.e., an overestimate) relative to the Reference analysis, and the CI_{95} doubles (Figure 2e). Ultimately, between the Reference analysis and NoMan the CI_{95} of $\overline{NBP}$ progressively increases to 105% relative to the Reference analysis (Figure 2e).

Partitioning of carbon fluxes between mean annual increments of C_{wood}, C_{som}, and $C_{DeadOrg}$ is more strongly dependent on assimilated biomass information (Figures 2b–2d and 2f–2h). At Duke Forest C_{wood} increment progressively decreases by 27% to ~3.1 Mg C ha^{-1} yr^{-1} and the CI_{95} increases 2.4-fold in NoMan. Meanwhile, $C_{DeadOrg}$ increment broadly decreases as information is removed from analyses; in the NoMan analysis the median increment is 34% smaller, while the CI_{95} is 10% smaller (Figure 2d). The median increment for C_{som} is largely unaffected by changes in assimilated data at Duke Forest, while the CI_{95} broadly increases (Figure 2c).

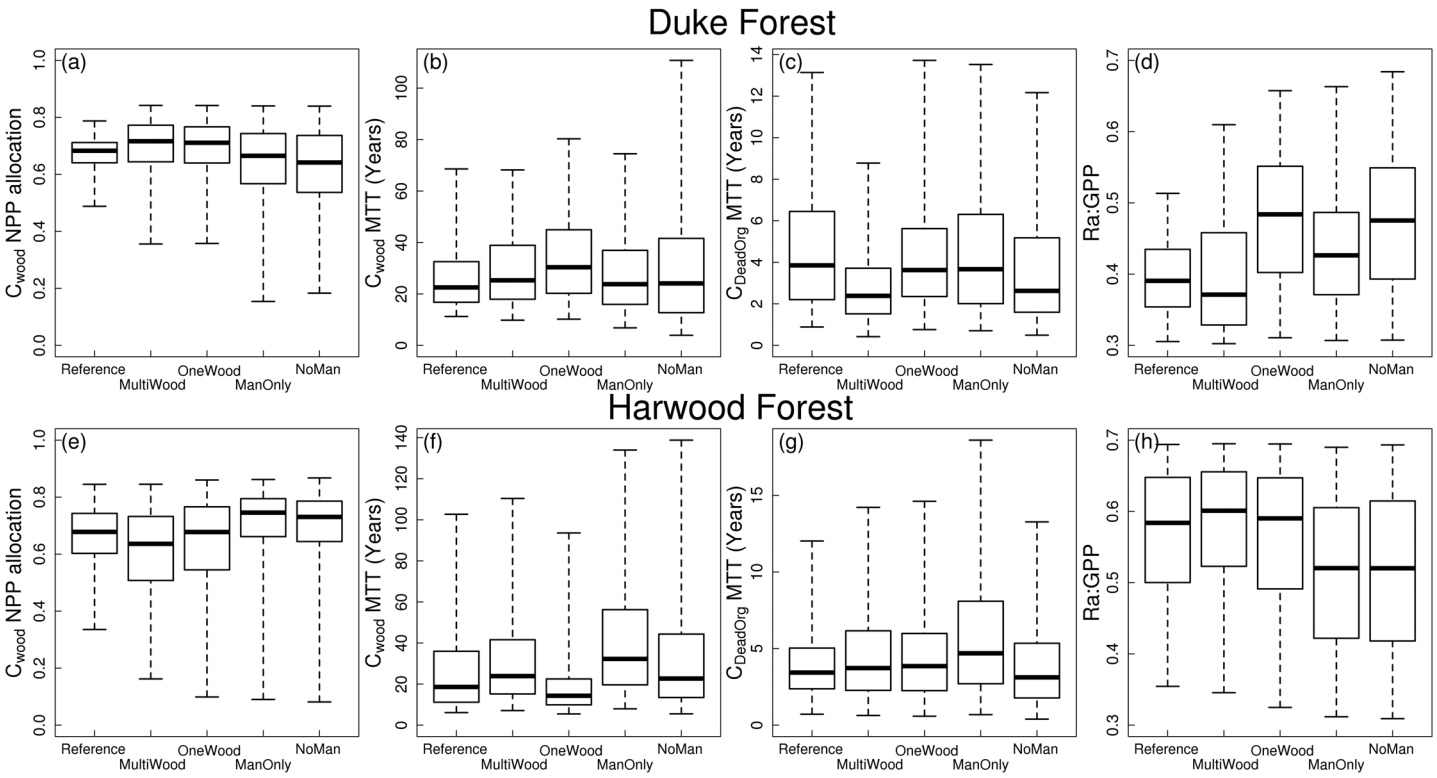

Figure 6. Box and whisker plots show the median and distribution information retrieved for key ecosystem traits at (a–d) Duke and (e–h) Harwood Forests. The median is shown by the thick black horizontal line, while the box and whiskers represent the 50% and 95% confidence intervals, respectively.

At Harwood Forest C_{wood} increment decreases in stages between the Reference analysis and OneWood (Figure 2f). In contrast to Duke Forest, the removal of all assimilated biomass stocks in ManOnly increases the C_{wood} increment by 70%, while the CI_{95} is more than double the Reference analysis. $C_{DeadOrg}$ is not substantially impacted at Harwood Forest, but the largest bias in the median estimate and CI_{95} compared to the Reference analysis is found when planting date only is used in ManOnly (Figure 2h). The C_{som} increment CI_{95} is greatest when only a single wood stock observation is assimilated in OneWood, while the median retrieval varies by

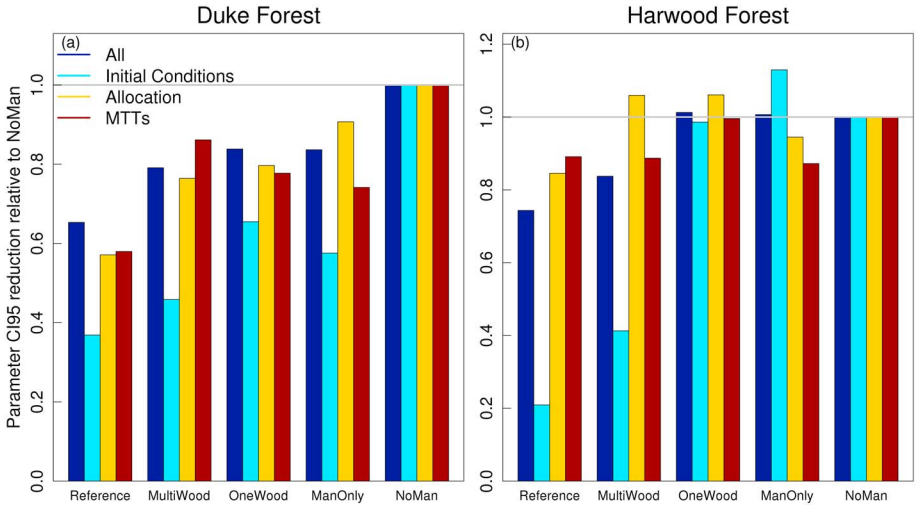

Figure 7. The proportional reduction of the 95% confidence interval for retrieved ecosystem traits for each analysis relative to the NoMan analysis. Information is presented for all retrieved traits as well as specific groupings related to the initial conditions, allocation of photosynthate, and mean transit times (MTTs). A value <1 indicates that the average constraint of parameters is greater than the least assimilated information scenario, NoMan.

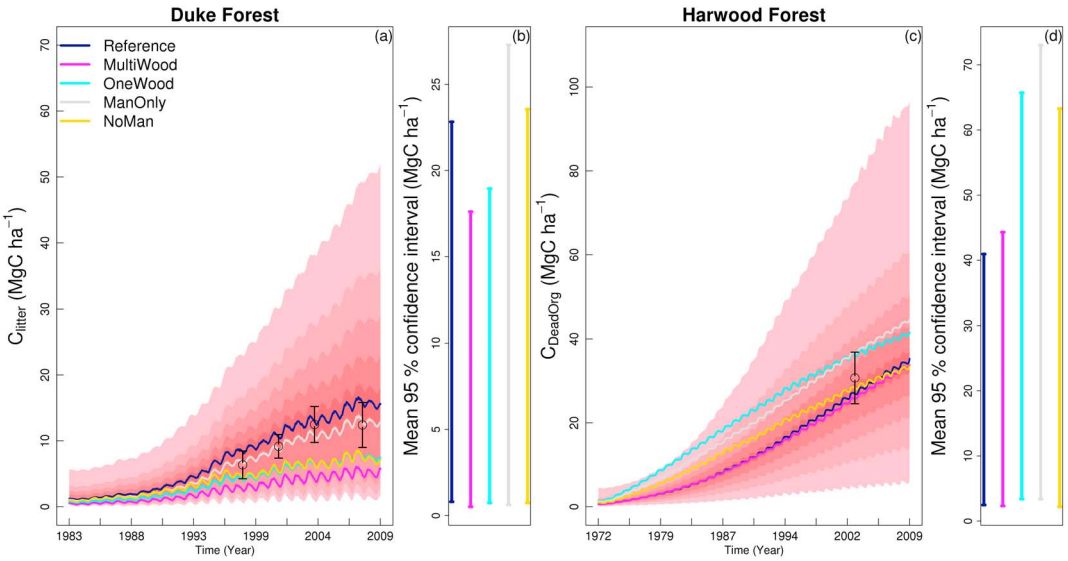

Figure 8. Time series of (a, b) C_{litter} at Duke Forest and (c, d) $C_{DeadOrg}$ (i.e., litter + coarse woody debris) at Harwood Forest. The shaded red area denotes the 95% confidence interval of the Reference analysis. The lines in Figures 8a and 8c are the ensemble medians for each of the experiments. The error bars shown in Figures 8b and 8d are the mean 95% confidence intervals for each experiment over the analysis period. Observations shown in unfilled black circles were not assimilated in any analysis.

<0.2 Mg C ha^{-1} yr^{-1} among analyses. It is important to note that overlap exists between the CI_{95} of the Reference and each of the reduced information analyses indicating that our "best" estimate of the carbon cycle is encompassed at all times.

3.2.2. C Stocks

The evolution of the C_{wood} pool over time is sensitive to reducing in situ biomass and management information particularly at Harwood Forest (Figure 3). At Harwood Forest when only one wood stock observation is assimilated (OneWood) the accumulation of carbon in C_{wood} shifts to front load the majority of the C_{wood} accumulation to the first half of the analysis (Figure 3h). This front loading increases the error between the analysis median and in situ wood stocks (Table 4). When multiple in situ woody observations are assimilated (MultiWood), the RMSE and bias are impacted by less than 2 Mg C ha^{-1} at either site compared to the Reference analysis. However, in OneWood, the RMSE at Duke Forest increases by 1.5-fold relative to the Reference analysis to 5.0 Mg C ha^{-1} and the magnitude of the bias increases by ~15-fold to −4.5 Mg C ha^{-1}. At Harwood Forest the OneWood RMSE increases by 95% to 8.6 Mg C ha^{-1} and the magnitude of the bias increases by

Table 4. Statistical Metrics, Root-Mean-Square Error (RMSE), and Mean Bias (Model-Obs), Between the Median Estimate of the Analysis Ensemble and Observed Estimates for C_{wood} (Mg C ha^{-1}) at Duke Forest and Harwood Forest[a]

Site	Scenario	RMSE	Bias	δ C_{wood} CI_{95}
Duke Forest	Reference	2.0	−0.29	–
	MultiWood	2.0	−0.31	2%
	OneWood	5.0	−4.58	−6%
	ManOnly	11.7	−11.4	211%
	NoMan	14.2	−13.4	230%
Harwood Forest	Reference	4.4	−0.21	–
	MultiWood	4.2	−0.43	−5%
	OneWood	8.6	8.05	48%
	ManOnly	39.9	34.3	169%
	NoMan	28.0	24.2	225%

[a]The δC_{wood} CI_{95} is the percentage change in the uncertainty of the C_{wood} pool at the end of the analysis relative to the Reference analysis.

39-fold to 8.05 Mg C ha^{-1}. Finally, the removal of all biomass observations results in large errors between the analysis medians and in situ wood stock observations (Table 4). The impact of including forest age information, thereby adding constraint to the initial C_{wood}, has little positive impact on long-term C_{wood} dynamics (Figures 3d, 3e, 3i, and 3j).

Analysis of foliar and fine root carbon stocks remains more challenging in all analyses but particularly at Harwood Forest (Figures 5a–5d). Each analysis at Duke Forest captures the magnitude and broad interannual variability of the foliar carbon stocks except the 2001 peak, as expected, given that the local LAI time series is assimilated in all scenarios (Figure 5a). The largest CI_{95} is found in NoMan when no biomass or management information are assimilated, and the smallest CI_{95} as expected is found in the Reference analysis. Fine root stocks are well simulated by all analyses with an error of less than 0.5 Mg C ha^{-1} except OneWood (Figure 5b). Similar to foliar stocks, the largest CI_{95} is found when no biomass or management information is assimilated with smaller uncertainties elsewhere (Figure 5b). At Harwood Forest the analyses are split between those which assimilated multiple wood stock observations (MultiWood and Reference) and those which do not (Figure 5c). Critically, no analysis was able to accurately simulate all of the observed foliar carbon stocks; the Reference and MultiWood analyses were able to accurately capture the observation from the 9 year old stand only. In contrast to Duke Forest, the CI_{95} decreases progressively as additional observations are assimilated with the largest decreases in CI_{95} occurring with the MultiWood and Reference analyses (Figure 5c). The fine root stock is substantially overestimated in all analyses by 1–2 Mg C ha^{-1} except in the Reference analysis, and uncertainties remain large in all analyses relative to the magnitude of the observed fine root stock. However, it should be noted that simulation of fine root stocks was also improved early in the analysis when repeated wood stock observations are assimilated in MultiWood (Figure 5d).

Assimilation of repeated woody biomass observations strongly constrains the state and CI_{95} of C_{litter} and $C_{DeadOrg}$ (Figure 8). At Duke Forest the median estimate for each analysis shows appropriate dynamics over time compared to the unassimilated observations (Figure 8). The smallest CI_{95} is found with the assimilation of repeated woody biomass observations (MultiWood), and the MultiWood analysis explains the largest proportion of variation in C_{litter} ($R^2 = 0.86$), however, the largest error (ensemble median observations) is also found in the MultiWood analysis (RMSE = 6.6 Mg C ha^{-1}). While only the median estimates of the Reference analysis and ManOnly overlap with the observation uncertainty, the CI_{95} of each analysis is large and encompasses each of the observations. At Harwood Forest the largest error between unassimilated observed $C_{DeadOrg}$ is jointly found in OneWood and ManOnly, while the largest CI_{95} is found in ManOnly (Figures 8c and 8d). The smallest error is found in the Reference, MultiWood, and NoMan analyses; however, the CI_{95} of NoMan is ~30% larger than either the Reference or MultiWood (Figures 8c and 8d).

3.2.3. Retrieved Ecosystem Traits

Ecosystem trait retrieval is highly sensitive to the in situ carbon stock and management information assimilated. At Duke Forest the median estimate and CI_{95} for the fraction of NPP allocated to C_{wood} are well constrained in the Reference analysis (Figure 6a). At Duke Forest the NPP allocation to C_{wood} is ~0.7 in all experiments, while the magnitude of the CI_{95} varies with assimilated information, peaking when only management information is included in NoMan (Figure 6a). Similarly, the largest CI_{95} and median estimates for $C_{DeadOrg}$ MTT is found in the NoMan analysis (Figure 6c). The retrieved C_{wood} MTT at Duke Forest is broadly consistent varying between 22 and 30 years but with the greatest CI_{95} found in NoMan (Figure 6b). The retrieved median estimate of Ra:GPP (CUE = 1 − Ra:GPP) varies among analyses, though the median estimate and the CI_{95} tend to increase as assimilated information is reduced, ultimately reaching ~0.5 in NoMan. At Harwood Forest the retrieved NPP allocation fraction is also ~0.7 and the largest uncertainty is found when repeated wood stock observations are removed (Figure 6e). The smallest CI_{95} and median estimate for C_{wood} MTT is found in OneWood; however, there is a broad pattern toward increasing uncertainties as information is removed from the analysis (Figure 6f). $C_{DeadOrg}$ MTT at Harwood Forest is less sensitive than at Duke Forest, with no substantial changes among analyses (Figure 6g). In contrast to Duke Forest, the retrieved Ra:GPP at Harwood Forest does not change substantially as long as biomass information is assimilated, although the CI_{95} progressively increases by ~10%. The Ra:GPP declines from ~0.6 to ~0.5 when all biomass information has been removed in ManOnly and NoMan (Figure 6h).

As expected there is an overall reduction in the uncertainty of retrieved ecosystem traits as assimilated information increases across both sites (Figure 7). At Duke Forest there is a broadly consistent trend of reducing overall uncertainty across all ecosystem traits, with the greatest reduction occurring with the inclusion of

management information and then with repeated woody biomass estimates (Figure 7a). While the degree of constraint on a given trait grouping (e.g., allocation of photosynthate or MTTs) varies between analyses, there is also an overall reduction of uncertainty across all groups. In contrast at Harwood Forest no substantial reduction in uncertainty occurs until repeated woody biomass information is assimilated in MultiWood, except for traits related to the allocation of photosynthate which remain poorly constrained (Figure 7b). Parameter correlations also vary widely between parameters and between sites. The mean of the absolute values of the Pearson's correlation coefficient is ~0.1 for both Duke and Harwood Forests. While the mean correlation coefficients are low, maximum coefficients achieved are >0.9 at both sites such as the negative correlation between C_{wood} turnover and the maximum rate of C_{labile} turnover at Duke Forest and the negative correlation between LCMA and Ra:GPP at Harwood Forest. However, there is no overall pattern in trait correlations between analyses at either site.

4. Discussion

4.1. Implications for Carbon Fluxes and Stocks

Our analyses demonstrate that assimilation of repeated woody biomass observations is not only able to constrain the overall carbon budget over multidecadal time periods but also the state and dynamics associated with dead organic matter contained in the litter and coarse woody debris (CWD). The $\overline{NBP}$ does not substantially vary between the Reference and MultiWood analyses at either site (Figures 2a and 2e). Constraint of $\overline{NBP}$ when assimilating repeated wood stock observations is achieved through additional constraint of the C_{wood} increment and also that of $C_{DeadOrg}$ and/or C_{som} mean annual increments. However, the CI_{95} for C_{som} stock remains substantial without in situ soil carbon information. The in situ soil carbon observations have lower uncertainty than that used here for the HWSD C_{som} prior, and unlike the HWSD the in situ information is well constrained in time. Therefore, using the HWSD in the absence of an understanding of uncertainties and temporal representation reduces the ability of our analysis to discriminate whether the soil is a net source or sink of carbon. The median and/or CI_{95} of the mean annual C_{wood} increment are sensitive to the assimilation of either a single or repeated wood stock observations (Figures 2b and 2f). The greatest impact can be seen at Harwood Forest where errors develop in the trajectory of the C_{wood} pool in the absence of repeated wood stock observations (Figures 3g–3j). Some of the strongest evidence for improved constraint using repeated wood stock estimates comes from the large reduction in uncertainty and/or bias in comparison with independent unassimilated observations of dead organic matter (i.e., C_{litter} and C_{cwd}) (Figure 8). This suggests that while future remote sensing missions such as NASA's global ecosystem dynamics investigating lidar (GEDI), which is expected to operate for ~1 year, will provide vital information characterizing the current state of the above ground biomass, multiyear missions, such as ESA's BIOMASS mission [*Le Toan et al.*, 2011], may have a greater potential to constrain unobserved components of the ecosystem carbon balance.

Our analysis generates estimates of GPP and R_{eco} at both sites which are consistent with independent estimates derived from eddy covariance [*Kowalski et al.*, 2004; *Stoy et al.*, 2006], thus providing a fully independent validation of the gross carbon fluxes in our analysis. The mean error between our analysis and the independent estimates (11–34%) are of a similar magnitude to the uncertainties associated with eddy covariance methodologies (~18% [*Stoy et al.*, 2006]). Moreover, the true uncertainty of the eddy covariance derived estimates of GPP and R_{eco} is likely to be much larger due to uncertainties in the flux partitioning methodologies [*Stoy et al.*, 2006; *Wehr et al.*, 2016].

When in situ carbon stock information is not assimilated (i.e., only forest age is known in ManOnly) the median increment of C_{wood} at both forests is biased leading to an overestimation of the $\overline{NBP}$ at Harwood Forest and an underestimation at Duke Forest. This also results in an equivalent error in the magnitude of C_{wood} (Figures 3d and 3i), although the increased width of the CI_{95} means that the majority of the in situ observations remain within the analysis uncertainty. However, such a large bias in C_{wood} stocks would lead to large errors in carbon fluxes associated with disturbance or projected harvest. Previous studies have identified the need for site-specific information such as stocking density [*Bellassen et al.*, 2011] or an indication of site fertility [*Bryars et al.*, 2013] to accurately simulate forest growth. Assimilation of in situ wood stock observations allows the analysis to infer these site-specific factors, particularly when planting age is known. Furthermore, these results highlight the potential value of repeated remotely sensed estimates of forest biomass [e.g., *Le Toan et al.*, 2011] and also of spatially explicit management data-based information such as forest yield class and soil properties, which may provide information on site-specific factors to correct errors demonstrated here.

Accurate analysis of the magnitude of soil and dead organic carbon stocks remains challenging. Significant uncertainty remains in the magnitude of the C_{som} (Figure 4) and $C_{DeadOrg}$ (Figure 8). The HWSD C_{som} prior does not significantly differ in magnitude from the in situ estimates at either site (Figure 4). Despite this, the impact of the HWSD prior is reduced due to a lack of a robust assessment of the uncertainty associated with the database and the lack of information on the time for which the priors are representative, necessitating a conserative use of the database. Additional effort should be made to improve the impact of such databases through development of a robust uncertainty analysis (currently lacking for the HWSD) and the inclusion of metadata providing information on temporal applicability. For dead organic matter which is dominated by coarse woody debris (CWD) the situation is more challenging, with no similar database of CWD stock estimates offering global coverage [*Magnusson et al.*, 2016]. However, given the good performance, particularly at Harwood Forest, in estimating $C_{DeadOrg}$ (Figure 8c), there is the potential for our system to generate accurate, though uncertain, spatially explicit estimates of litter and CWD. The dynamics of soil and dead organic carbon stocks have been identified as a key source of uncertainty in Earth System Models (ESMs) [*Brovkin et al.*, 2012; *Exbrayat et al.*, 2014a], particularly the difficulty in accurately describing transit times [*Todd-Brown et al.*, 2013] and the assumption of steady state removing sensitivity to initial conditions [*Brovkin et al.*, 2012; *Exbrayat et al.*, 2014b]. Recent efforts to improve the representation of soil decomposition processes, such as the explicit representation of microbial activity chemical composition, have highlighted that the commonly used first-order kinetic decomposition model (as used here) is insufficiently sensitive to changes in litter quality and too sensitive to litter quantity [*Wieder et al.*, 2013; *Xenakis and Williams*, 2014]. Therefore, future efforts should assess how additional constraints on soil carbon dynamics or magnitude can be inferred when using a more complex representation of soil processes.

4.2. Implications for Ecosystem Trait Retrieval

Our data assimilation analysis retrieves estimates for ecosystem traits that are consistent with field data. Retrieved LCMA estimates are consistent with in situ observations even without the assimilation of foliar carbon stock information, which is important given that LCMA is strongly correlated with other canopy traits such as nutrient status and leaf lifespan [*Wright et al.*, 2004; *Kattge et al.*, 2011]. The retrieved estimates of NPP allocation to wood and Ra:GPP at both sites is consistent with previous studies on temperate evergreen forests [*Wolf et al.*, 2011; *Chen et al.*, 2013]. Higher Ra:GPP values have been found to be associated with nutrient stress [*Chen et al.*, 2013] which is consistent with low-fertility peaty gley soils found at Harwood Forest. Even though the assimilation of increasing amounts of biomass information improved the constraint on Ra:GPP, this trait remains highly uncertain in all analyses (Figures 6d and 6h); Ra:GPP has been shown to vary with tree age, in addition to climate and environmental stress [*Maseyk et al.*, 2008; *Piao et al.*, 2010; *Dillaway and Kruger*, 2014; *Malhi et al.*, 2015]. Therefore, the current fixed ratio used in DALEC and other terrestrial ecosystem models [e.g., *Landsberg and Waring*, 1997; *Ostle et al.*, 2009] may the lack necessary structural complexity required to reduce retrieval uncertainty [*De Kauwe et al.*, 2014]. However, due to the simplicity of DALEC, our analysis framework could provide a viable approach to implement and test current hypotheses of NPP allocation and Ra:GPP [e.g., *Franklin et al.*, 2012].

Accurate estimation of ecosystem transit times remains challenging, necessitating greater integration with experimental field studies to improve process representation [e.g., *De Kauwe et al.*, 2014; *Malhi et al.*, 2015]. In the Reference analysis at Duke Forest the magnitude of the wood pool, its dynamics, and NPP allocation patterns closely agree with independent field-based estimates. In contrast, the mean transit times estimated here for wood are ~100 years shorter than field estimates [*De Kauwe et al.*, 2014]. DALEC lacks an explicit representation of self-thinning which becomes increasingly important as trees increase in height [*Lonsdale et al.*, 2015]. In DALEC self-thinning is included implicitly in the retrieved woody transit time, potentially explaining this discrepancy. Furthermore, we also show substantial reduction in the uncertainty of traits related to the allocation of photosynthate, MTTs, and initial conditions of carbon stocks, particularly with the assimilation of repeated woody biomass information (Figure 7). Each of these components have been highlighted as important uncertainties when attempting to generate robust estimates of how the terrestrial carbon cycle will respond to predicted future climate change [*Todd-Brown et al.*, 2013; *Exbrayat et al.*, 2014b; *Reich et al.*, 2014]. Our analysis highlights the remaining challenges in fully constraining ecosystem traits. These challenges introduce substantial uncertainties when attempting to predict the response of the terrestrial carbon cycle across landscapes under future climate change [*Richardson et al.*, 2013b; *Friend et al.*, 2014].

4.3. Conclusions

Here we have demonstrated the critical role of repeated woody biomass estimates in constraining the dynamics of the major ecosystem carbon pools (i.e., woody biomass, dead organic matter, and soil organic matter) and net biome production and, therefore, the potential benefit of future remote sensing programs. Moreover, we show that increasing assimilation of biomass observations successfully reduces bias and overall uncertainty in retrieved ecosystem traits including those governing the initial conditions, allocation of NPP, and ecosystem turnover rates including soil carbon. However, we also show that there remains significant challenges in accurately estimating the magnitude of ecosystem carbon stocks, in particular soil organic matter, necessitating additional effort in utilizing soil inventories and model structural development.

Acknowledgments

This work was funded primarily through the NERC GHG program GREENHOUSE project (grant NE/K002619/1). Additional resources were provided by GEOCARBON and the NERC National Centre for Earth Observations (NCEO). Contribution by A.A.B. was carried out at the Jet Propulsion Laboratory, California Institute of Technology, under a contract with the National Aeronautics and Space Administration. This work has made use of the resources provided by the Edinburgh Compute and Data Facility (ECDF) (http://www.ecdf.ed.ac.uk/). Source code and parameters for the DALEC C-cycle model are available on request from the authors (t.l.smallman@ed.ac.uk). All field observations used here for Duke Forest were provided by Heather McCarthy (heather.mccarthy@ou.edu) and Ram Oren (ramoren@duke.edu) whom the authors wish to thank. Research at Duke Forest was supported by the Office of Science (BER), U.S. Department of Energy, through contract DE-AC02-98CH10886 with Brookhaven National Laboratory and grant DE-FG02-95ER62083 with Duke University. The Harwood Forest data collection was supported by the CARBO-AGE project (contract ENV4-CT97-0577), funded by the EC Fifth Framework Environment and Climate Research Programme. The Harwood Forest data were provided by and are available from Mauricio Mencuccini (m.mencuccini@ed.ac.uk). The MODIS LAI data were freely downloaded from NASA (http://reverb.echo.nasa.gov/reverb/). The Harmonized World Soil Database (HWSD) was compiled by IIASA and FAO and is freely available (http://webarchive.iiasa.ac.at/Research/LUC/External-World-soil-database/HTML/). The Princeton meteorological drivers used in this analysis were freely downloaded from the Terrestrial Hydrology Research Group website (http://hydrology.princeton.edu/data.pgf.php).

References

Akers, M. K., M. Kane, D. Zhao, R. O. Teskey, and R. F. Daniels (2013), Effects of planting density and cultural intensity on stand and crown attributes of mid-rotation loblolly pine plantations, *For. Ecol. Manage.*, *310*, 468–475, doi:10.1016/j.foreco.2013.07.062.

Albaugh, T. J., H. L. Allen, P. M. Dougherty, and K. H. Johnsen (2004), Long term growth responses of loblolly pine to optimal nutrient and water resource availability, *For. Ecol. Manage.*, *192*(1), 3–19, doi:10.1016/j.foreco.2004.01.002.

Avitabile, V., et al. (2016), An integrated pan-tropical biomass map using multiple reference datasets, *Global Change Biol.*, *22*(4), 1406–1420, doi:10.1111/gcb.13139.

Bellassen, V., G. Le Maire, O. Guin, J. F. Dhote, P. Ciais, and N. Viovy (2011), Modelling forest management within a global vegetation model—Part 2: Model validation from a tree to a continental scale, *Ecol. Modell.*, *222*(1), 57–75, doi:10.1016/j.ecolmodel.2010.08.038.

Black, K., et al. (2009), Carbon stock and stock changes across a Sitka spruce chronosequence on surface-water gley soils, *Forestry*, *82*(3), 255–272, doi:10.1093/forestry/cpp005.

Bloom, A. A., and M. Williams (2015), Constraining ecosystem carbon dynamics in a data-limited world: Integrating ecological "common sense" in a model-data-fusion framework, *Biogeosciences*, *12*, 1299–1315, doi:10.5194/bg-12-1299-2015.

Bloom, A. A., J.-F. Exbrayat, I. R. van der Velde, L. Feng, and M. Williams (2016), The decadal state of the terrestrial carbon cycle: Global retrievals of terrestrial carbon allocation, pools, and residence times, *Proc. Natl. Acad. Sci. U.S.A.*, *113*(5), 1285–1290, doi:10.1073/pnas.1515160113.

Brovkin, V., P. M. van Bodegom, T. Kleinen, C. Wirth, W. K. Cornwell, J. H. C. Cornelissen, and J. Kattge (2012), Plant-driven variation in decomposition rates improves projections of global litter stock distribution, *Biogeosciences*, *9*(1), 565–576, doi:10.5194/bg-9-565-2012.

Bryars, C., C. Maier, D. Zhao, M. Kane, B. Borders, R. Will, and R. Teskey (2013), Fixed physiological parameters in the 3-PG model produced accurate estimates of loblolly pine growth on sites in different geographic regions, *For. Ecol. Manage.*, *289*, 501–514, doi:10.1016/j.foreco.2012.09.031.

Carter, M. C., and C. D. Foster (2006), Milestones and millstones: A retrospective on 50 years of research to improve productivity in loblolly pine plantations, *For. Ecol. Manage.*, *227*(1–2), 137–144, doi:10.1016/j.foreco.2006.02.014.

Carvalhais, N., et al. (2014), Global covariation of carbon turnover times with climate in terrestrial ecosystems, *Nature*, *514*(7521), 213–217, doi:10.1038/nature13731.

Chen, G., Y. Yang, and D. Robinson (2013), Allocation of gross primary production in forest ecosystems: Allometric constraints and environmental responses, *New Phytol.*, *200*(4), 1176–1186, doi:10.1111/nph.12426.

De Kauwe, M. G., et al. (2014), Where does the carbon go? A model-data intercomparison of vegetation carbon allocation and turnover processes at two temperate forest free-air CO_2 enrichment sites, *New Phytol.*, *203*(3), 883–899, doi:10.1111/nph.12847.

Dillaway, D. N., and E. L. Kruger (2014), Trends in seedling growth and carbon-use efficiency vary among broadleaf tree species along a latitudinal transect in eastern North America, *Global Change Biol.*, *20*(3), 908–922.

Exbrayat, J. F., A. J. Pitman, and G. Abramowitz (2014a), Disentangling residence time and temperature sensitivity of microbial decomposition in a global soil carbon model, *Biogeosciences*, *11*(23), 6999–7008, doi:10.5194/bg-11-6999-2014.

Exbrayat, J. F., A. J. Pitman, and G. Abramowitz (2014b), Response of microbial decomposition to spin-up explains CMIP5 soil carbon range until 2100, *Geosci. Model Dev.*, *7*(6), 2683–2692, doi:10.5194/gmd-7-2683-2014.

Franklin, O., J. Johansson, R. C. Dewar, U. Dieckmann, R. E. McMurtrie, A. Brannstrom, and R. Dybzinski (2012), Modeling carbon allocation in trees: A search for principles, *Tree Physiol.*, *32*(6), 648–666, doi:10.1093/treephys/tpr138.

Friend, A. D., et al. (2014), Carbon residence time dominates uncertainty in terrestrial vegetation responses to future climate and atmospheric CO_2, *Proc. Natl. Acad. Sci. U.S.A.*, *111*(9), 3280–3285, doi:10.1073/pnas.1222477110.

Gough, C. M., C. E. Flower, C. S. Vogel, D. Dragoni, and P. S. Curtis (2009), Whole-ecosystem labile carbon production in a north temperate deciduous forest, *Agric. For. Meteorol.*, *149*(9), 1531–1540, doi:10.1016/j.agrformet.2009.04.006.

Hansen, M. C. et al. (2013), High-resolution global maps of 21st-century forest cover change, *Science*, *342*(6160), 850–853, doi:10.1126/science.1244693.

Hiederer, R., and M. Kochy, (2011), Global soil organic carbon estimates and the Harmonized World Soil Database, *EUR 25225 EN – EUR Sci. Tech. Res. Ser.*, 79 pp., Publ. Office of the European Union.

Jarvis, P. G., R. J. Clement, J. Grace, and K. A. Smith (2009), The role of forests in the capture and exchange of energy and greenhouse gases, in *Combating Climate Change: A Role for UK Forests. An Assessment of the Potential of the UK Trees and Woodlands to Mitigate and Adapt to Climate Change*, edited by D. J. Read et al., pp. 21–47, TSO, Edinburgh.

Jiang, L., Y. Yan, O. Hararuk, N. Mikle, J. Xia, Z. Shi, J. Tjiputra, T. Wu, and Y. Luo (2015), Scale-dependent performance of CMIP5 earth system models in simulating terrestrial vegetation carbon*, *J. Clim.*, *28*(13), 5217–5232, doi:10.1175/JCLI-D-14-00270.1.

Jolly, W. M., R. Nemani, and S. W. Running (2005), A generalized, bioclimatic index to predict foliar phenology in response to climate, *Global Change Biol.*, *11*(4), 619–632, doi:10.1111/j.1365-2486.2005.00930.x.

Kattge, J., et al. (2011), TRY—A global database of plant traits, *Global Change Biol.*, *17*(9), 2905–2935, doi:10.1111/j.1365-2486.2011.02451.x.

Kowalski, A. et al. (2004), Paired comparisons of carbon exchange between undisturbed and regenerating stands in four managed forests in Europe, *Global Change Biol.*, *10*(10), 1707–1723, doi:10.1111/j.1365-2486.2004.00846.x.

Kuppel, S., P. Peylin, F. Chevallier, C. Bacour, F. Maignan, and A. D. Richardson (2012), Constraining a global ecosystem model with multi-site eddy-covariance data, *Biogeosciences*, *9*(10), 3757–3776, doi:10.5194/bg-9-3757-2012.

Landsberg, J. J., and R. H. Waring (1997), A generalised model of forest productivity using simplified concepts of radiation-use efficiency, carbon balance and partitioning, *For. Ecol. Manage.*, *95*(3), 209–228, doi:10.1016/S0378-1127(97)00026-1.

Le Quéré, C., et al. (2015), Global carbon budget 2015, *Earth Syst. Sci. Data*, *7*(2), 349–396, doi:10.5194/essd-7-349-2015.
Le Toan, T., et al. (2011), The BIOMASS mission: Mapping global forest biomass to better understand the terrestrial carbon cycle, *Remote Sens. Environ.*, *115*(11, SI), 2850–2860, doi:10.1016/j.rse.2011.03.020.
Lichter, J., S. A. Billings, S. E. Ziegler, D. Gaindh, R. Ryals, A. C. Finzi, R. B. Jackson, E. A. Stemmler, and W. H. Schlesinger (2008), Soil carbon sequestration in a pine forest after 9 years of atmospheric CO_2 enrichment, *Global Change Biol.*, *14*(12), 2910–2922, doi:10.1111/j.1365-2486.2008.01701.x.
Liu, Y. Y., A. I. J. M. van Dijk, R. A. M. de Jeu, J. G. Canadell, M. F. McCabe, J. P. Evans, and G. Wang (2015), Recent reversal in loss of global terrestrial biomass, *Nat. Clim. Change*, *5*(5), 470–474, doi:10.1038/NCLIMATE2581.
Lonsdale, J., G. Xenakis, M. Mencuccini, and M. Perks (2015), A comparison of models for quantifying growth and standing carbon in UK Scots pine forests, *iForest – Biogeosci. For.*, *8*, 596–605, doi:10.3832/ifor1403-008.
Luyssaert, S., et al. (2007), CO_2 balance of boreal, temperate, and tropical forests derived from a global database, *Global Change Biol.*, *13*(12), 2509–2537, doi:10.1111/j.1365-2486.2007.01439.x.
Luyssaert, S., et al. (2010), The European carbon balance. Part 3: Forests, *Global Change Biol.*, *16*(5), 1429–1450, doi:10.1111/j.1365-2486.2009.02056.x.
Magnani, F., et al. (2007), The human footprint in the carbon cycle of temperate and boreal forests, *Nature*, *447*, 849–851, doi:10.1038/nature05847.
Magnusson, R. I., A. Tietema, J. H. C. Cornelissen, M. M. Hefting, and K. Kalbitz (2016), Tamm Review: Sequestration of carbon from coarse woody debris in forest soils, *For. Ecol. Manage.*, *377*, 1–15, doi:10.1016/j.foreco.2016.06.033.
Malhi, Y., et al. (2015), The linkages between photosynthesis, productivity, growth and biomass in lowland Amazonian forests, *Global Change Biol.*, *21*(6), 2283–2295, doi:10.1111/gcb.12859.
Maseyk, K., J. M. Grunzweig, E. Rotenberg, and D. Yakir (2008), Respiration acclimation contributes to high carbon-use efficiency in a seasonally dry pine forest, *Global Change Biol.*, *14*(7), 1553–1567, doi:10.1111/j.1365-2486.2008.01604.x.
McCarthy, H. R., R. Oren, A. C. Finzi, D. S. Ellsworth, H.-S. Kim, K. H. Johnsen, and B. Millar (2007), Temporal dynamics and spatial variability in the enhancement of canopy leaf area under elevated atmospheric CO_2, *Global Change Biol.*, *13*(12), 2479–2497, doi:10.1111/j.1365-2486.2007.01455.x.
McCarthy, H. R., et al. (2010), Re-assessment of plant carbon dynamics at the Duke free-air CO_2 enrichment site: Interactions of atmospheric [CO_2] with nitrogen and water availability over stand development, *New Phytol.*, *185*(2), 514–528, doi:10.1111/j.1469-8137.2009.03078.x.
Morison, J., R. Matthews, G. Miller, M. Perks, T. Randle, E. Vanguelova, M. White, and S. Yamulki, (2012), *Forestry Commission Res. Rep.*, pp. 1–149, Forestry Commission, Edinburgh.
National Forest Inventory (2011a), *National Forest Inventory Woodland Area Statistics: Scotland*, Forestry Commission statistical release, Forestry Commission, EH12 7AT, Edinburgh.
National Forest Inventory (2011b), *Standing Timber Volume for Coniferous Trees in Britain*, Forestry Commission statistical release, Forestry Commission, EH12 7AT, Edinburgh.
Oren, R., et al. (2001), Soil fertility limits carbon sequestration by forest ecosystems in a CO_2-enriched atmosphere, *Nature*, *411*(6836), 469–472, doi:10.1038/35078064.
Oren, R., C. Hseih, P. Stoy, J. Albertson, H. McCarthy, P. Harrell, and G. Katul (2006), Estimating the uncertainty in annual net ecosystem carbon exchange: Spatial variation in turbulent fluxes and sampling errors in eddy-covariance measurements, *Global Change Biol.*, *12*(5), 883–896, doi:10.1111/j.1365-2486.2006.01131.x.
Ostle, N. J., et al. (2009), Integrating plant-soil interactions into global carbon cycle models, *J. Ecol.*, *97*(5), 851–863, doi:10.1111/j.1365-2745.2009.01547.x.
Pan, Y., et al. (2011), A large and persistent carbon sink in the world's forests, *Science*, *333*(6045), 988–993, doi:10.1126/science.1201609.
Piao, S., S. Luyssaert, P. Ciais, I. A. Janssens, A. Chen, C. Cao, J. Fang, P. Friedlingstein, Y. Luo, and S. Wang (2010), Forest annual carbon cost: A global-scale analysis of autotrophic respiration, *Ecology*, *91*(3), 652–661, doi:10.1890/08-2176.1.
Poorter, L., et al. (2016), Biomass resilience of Neotropical secondary forests, *Nature*, *7589*(530), 211–214, doi:10.1038/nature16512.
Randle, T. J., and T. A. R. Jenkins (2011), *The Construction of Lookup Tables for Estimating Changes in Carbon Stocks in Forestry Projects: A Background Document for Users of the Forestry Commission's Woodland Carbon Code*, Forestry Commission, U. K.
Reich, P. B., R. L. Rich, X. Lu, Y.-P. Wang, and J. Oleksyn (2014), Biogeographic variation in evergreen conifer needle longevity and impacts on boreal forest carbon cycle projections, *Proc. Natl. Acad. Sci. U.S.A.*, *111*(38), 13,703–13,708, doi:10.1073/pnas.1216054110.
Richardson, A. D., M. S. Carbone, T. F. Keenan, C. I. Czimczik, D. Y. Hollinger, P. Murakami, P. G. Schaberg, and X. Xu (2013a), Seasonal dynamics and age of stemwood nonstructural carbohydrates in temperate forest trees, *New Phytol.*, *197*(3), 850–861, doi:10.1111/nph.12042.
Richardson, A. D., T. F. Keenan, M. Migliavacca, Y. Ryu, O. Sonnentag, and M. Toomey (2013b), Climate change, phenology, and phenological control of vegetation feedbacks to the climate system, *Agric. For. Meteorol.*, *169*, 156–173, doi:10.1016/j.agrformet.2012.09.012.
Richardson, A. D., M. S. Carbone, B. A. Huggett, M. E. Furze, C. I. Czimczik, J. C. Walker, X. Xu, P. G. Schaberg, and P. Murakami (2015), Distribution and mixing of old and new nonstructural carbon in two temperate trees, *New Phytol.*, *206*(2), 590–597, doi:10.1111/nph.13273.
Saatchi, S. S., et al. (2011), Benchmark map of forest carbon stocks in tropical regions across three continents, *Proc. Natl. Acad. Sci. U.S.A.*, *108*(24), 9899–9904, doi:10.1073/pnas.1019576108.
Samuelson, L. J., K. Johnsen, and T. Stokes (2004), Production, allocation, and stemwood growth efficiency of Pinus taeda L. stands in response to 6 years of intensive management, *Forest Ecol. Manage.*, *192*(1), 59–70, doi:10.1016/j.foreco.2004.01.005.
Sheffield, J., G. Goteti, and E. F. Wood (2006), Development of a 50-year high-resolution global dataset of meteorological forcings for land surface modeling, *J. Clim.*, *19*(13), 3088–3111, doi:10.1175/JCLI3790.1.
Sierra, C. A., M. Mller, H. Metzler, S. Manzoni, and S. E. Trumbore (2016), The muddle of ages, turnover, transit, and residence times in the carbon cycle, *Global Change Biol.*, doi:10.1111/gcb.13556, in press.
Smith, M. J., D. W. Purves, M. C. Vanderwel, V. Lyutsarev, and S. Emmott (2013), The climate dependence of the terrestrial carbon cycle, including parameter and structural uncertainties, *Biogeosciences*, *10*(1), 583–606, doi:10.5194/bg-10-583-2013.
Stoeckli, R., T. Rutishauser, D. Dragoni, J. O'Keefe, P. E. Thornton, M. Jolly, L. Lu, and A. S. Denning (2008), Remote sensing data assimilation for a prognostic phenology model, *J. Geophys. Res. Biogeosci.*, *113*, G04021, doi:10.1029/2008JG000781.
Stoy, P. C., G. G. Katul, M. B. S. Siqueira, J.-Y. Juang, K. A. Novick, J. M. Uebelherr, and R. Oren (2006), An evaluation of models for partitioning eddy covariance-measured net ecosystem exchange into photosynthesis and respiration, *Agric. For. Meteorol.*, *141*(1), 2–18, doi:10.1016/j.agrformet.2006.09.001.

Thurner, M., C. Beer, M. Santoro, N. Carvalhais, T. Wutzler, D. Schepaschenko, A. Shvidenko, E. Kompter, B. Ahrens, S. R. Levick, and C. Schmullius (2014), Carbon stock and density of northern boreal and temperate forests, *Global Ecol. Biogeogr.*, *23*(3), 297–310, doi:10.1111/geb.12125.

Tian, H., et al. (2015), Global patterns and controls of soil organic carbon dynamics as simulated by multiple terrestrial biosphere models: Current status and future directions, *Global Biogeochem. Cycles*, *29*(6), 775–792, doi:10.1002/2014GB005021.

Todd-Brown, K. E. O., J. T. Randerson, W. M. Post, F. M. Hoffman, C. Tarnocai, E. A. G. Schuur, and S. D. Allison (2013), Causes of variation in soil carbon simulations from CMIP5 earth system models and comparison with observations, *Biogeosciences*, *10*(3), 1717–1736, doi:10.5194/bg-10-1717-2013.

US Forest Service (2001), U.S. forest facts and historical trends, *Tech. Rep.*, USDA Forest Service, National Office, Arlington, Va.

Wehr, R., J. W. Munger, J. B. McManus, D. D. Nelson, M. S. Zahniser, E. A. Davidson, S. C. Wofsy, and S. R. Saleska (2016), Seasonality of temperate forest photosynthesis and daytime respiration, *Nature*, *534*(7609), 680–683, doi:10.1038/nature17966.

Wieder, W. R., G. B. Bonan, and S. D. Allison (2013), Global soil carbon projections are improved by modelling microbial processes, *Nat. Clim. Change*, *3*(10), 909–912, doi:10.1038/NCLIMATE1951.

Williams, M., P. A. Schwarz, B. E. Law, J. Irvine, and M. Kurpius (2005), An improved analysis of forest carbon dynamics using data assimilation, *Global Change Biol.*, *11*, 89–105.

Williams, M., E. Rastetter, D. Fernandes, M. Goulden, G. Shaver, and L. Johnson (1997), Predicting gross primary productivity in terrestrial ecosystems, *Ecol. Appl.*, *7*(3), 882–894.

Wolf, A., C. B. Field, and J. A. Berry (2011), Allometric growth and allocation in forests: A perspective from FLUXNET, *Ecol. Appl.*, *21*(5), 1546–1556.

Wright, I. J., et al. (2004), The worldwide leaf economics spectrum, *Nature*, *428*(6985), 821–827, doi:10.1038/nature02403.

Xenakis, G., and M. Williams (2014), Comparing microbial and chemical kinetics for modelling soil organic carbon decomposition using the DecoChem v1.0 and DecoBio v1.0 models, *Geosci. Model Dev.*, *7*(4), 1519–1533, doi:10.5194/gmd-7-1519-2014.

Zerva, A., and M. Mencuccini (2005), Carbon stock changes in a peaty gley soil profile after afforestation with Sitka spruce (Picea sitchensis), *Ann. For. Sci.*, *62*, 873–880.

Ziehn, T., M. Scholze, and W. Knorr (2012), On the capability of Monte Carlo and adjoint inversion techniques to derive posterior parameter uncertainties in terrestrial ecosystem models, *Global Biogeochem. Cycles*, *26*(3), GB3025, doi:10.1029/2011GB004185.